

Efficient Model-Based Reinforcement Learning for Robot Control via Online Learning

Fang Nan¹, Hao Ma^{2,3}, Qinghua Guan⁴, Josie Hughes⁴, Michael Muehlebach², and Marco Hutter¹

Journal Title
XX(X):1–16
©The Author(s) 2016
Reprints and permission:
sagepub.co.uk/journalsPermissions.nav
DOI: 10.1177/ToBeAssigned
www.sagepub.com/

SAGE

Abstract

We present an online model-based reinforcement learning algorithm suitable for controlling complex robotic systems directly in the real world. Unlike prevailing sim-to-real pipelines that rely on extensive offline simulation and model-free policy optimization, our method builds a dynamics model from real-time interaction data and performs policy updates guided by the learned dynamics model. This efficient model-based reinforcement learning scheme significantly reduces the number of samples to train control policies, enabling direct training on real-world rollout data. This significantly reduces the influence of bias in the simulated data, and facilitates the search for high-performance control policies. We adopt online learning analysis to derive sublinear regret bounds under standard stochastic online optimization assumptions, providing formal guarantees on performance improvement as more interaction data are collected. Experimental evaluations were performed on a hydraulic excavator arm and a soft robot arm, where the algorithm demonstrates strong sample efficiency compared to model-free reinforcement learning methods, reaching comparable performance within hours. Robust adaptation to shifting dynamics was also observed when the payload condition was randomized. Our approach paves the way toward efficient and reliable on-robot learning for a broad class of challenging control tasks.

Keywords

Class file, $\text{\LaTeX} 2_{\mathcal{E}}$, SAGE Publications

Introduction

In recent years, Reinforcement Learning (RL) has achieved remarkable success across a variety of robotic tasks, ranging from manipulation (Kroemer et al. 2021) and locomotion Miki et al. (2022) to aerial vehicle control (Kaufmann et al. 2023). By leveraging neural networks and end-to-end learning algorithms, agents can acquire policies that directly map high-dimensional sensor inputs to low-level motor commands (Lin et al. 2025).

The prevailing RL workflow in robotics today typically follows a sim-to-real paradigm. In this pipeline, control policies are first trained extensively in physical simulators to gather large amounts of data. After achieving satisfying performance in simulation, the policies are transferred to physical robots and used in real-world applications. This approach has been widely adopted due to its ability to leverage the efficiency of simulation for data collection, allowing for rapid iteration and exploration of complex environments. In particular, popular model-free RL algorithms, such as Proximal Policy Optimization (PPO) (Schulman et al. 2017), require large amounts of data to effectively train control policies, making data collection in simulation an indispensable step.

This sim-to-real pipeline, however, comes with significant limitations. First, the fidelity of simulators is often insufficient to capture the nuanced dynamics of complex robotic hardware, leading to a sim-to-real gap that degrades performance when policies are deployed in the real world. In some cases, researchers have reported that RL algorithms

exploit the simulator’s imperfections and learn policies that cannot be transferred to the real world (Kadian et al. 2020). A number of strategies have been proposed to mitigate this issue, such as domain randomization (Tobin et al. 2017), real-to-sim (Villasevil et al. 2024), and domain adaptation (Kumar et al. 2021). While these methods can improve the transferability of policies, extensive tuning effort and a careful tradeoff between performance and robustness are often required.

The applicability of the sim-to-real paradigm is further limited by the lack of simulators for complex robotic systems. Robotic platforms with hydraulic or pneumatic actuators, deformable soft structures, or robots that interact with non-rigid objects have distinct applications and are vital for many real-world tasks. Existing simulators for robot learning, while being very efficient in simulating rigid-body systems with torque-controlled joints, have minimal support for these complex systems (Makoviychuk et al. 2021).

¹Robotic Systems Lab, ETH Zürich, Zürich, Switzerland

²Learning and Dynamical Systems, Max Planck Institute for Intelligent Systems, Tübingen, Germany

³Institute for Dynamic Systems and Control, ETH Zürich, Zürich, Switzerland

⁴CREATE Lab, EPFL, Lausanne, Switzerland

Corresponding author:

Fang Nan, Robotic Systems Lab, ETH Zürich, Leonhardstrasse 21, 8092 Zürich, Switzerland.

Email: fannan@ethz.ch

Although specialized simulators exist for such multidomain physical simulation (The MathWorks Inc. 2025; Algoryx Simulation AB 2025), their efficiency is not sufficient for parallelized data collection in robot learning applications.

These limitations of the sim-to-real paradigm motivate alternative RL algorithms that can operate directly on physical robots, and model-based RL methods have therefore emerged as a promising approach. Unlike model-free methods, model-based RL algorithms learn a dynamics model of the environment and use the model to plan actions or improve a policy. As the model learning can be performed with off-policy data, these methods can significantly reduce the amount of real-world data required for training. Existing model-based RL algorithms, however, have disadvantages in terms of algorithm efficiency, making them hard to deploy in real-world learning settings (Romero et al. 2025).

Contributions

To address the limitations mentioned above, we propose a novel model-based RL algorithm designed for online training directly on physical robots. Our approach constructs a dynamics model from real-time interaction data and uses the learned dynamics model to generate approximate gradients for policy optimization on real-world data. This paradigm significantly reduces the need for generating a large amount of synthetic data during policy optimization or online planning, thus achieving faster convergence and lower computational cost. Moreover, by operating entirely on data collected on the real system, our method gracefully handles unmodeled phenomena, thus extending applicability to robots with complex or partially unknown dynamics.

We support the proposed approach with theoretical analysis from the perspective of stochastic online optimization. In particular, we analyze regret of the online model and policy learning modules in the proposed method under some simplifications and discuss necessary conditions for joint convergence.

Finally, we demonstrate the efficacy of our method through experiments on two robotic platforms: a hydraulic excavator arm (HEAP) and a modular soft robot arm. The real-world experiments show that our method achieves strong sample efficiency toward learning control policies, enabling RL directly on physical robots.

The remainder of the paper is organized as follows. Section 2 reviews related work in model-based and model-free RL, with an emphasis on their application to robot control problems. Section 3 formalizes the problem setting, introduces our online learning framework, and presents the theoretical analysis leading to regret bounds. Section 4 details our experimental setup on multiple robotic platforms. Section 5 reports empirical results, comparing against state-of-the-art baselines. Finally, Section 6 concludes with a discussion of limitations and future directions.

Related Work

Model-based RL in Robotics

RL has shown great performance in various robotic applications. In particular, model-free RL has become the dominant approach for training control policies for legged

locomotion (Miki et al. 2022). Other successful examples include racing drones (Kaufmann et al. 2023), robotic manipulation (Kroemer et al. 2021), and control of agile robotic systems (Ma et al. 2023; Büchler et al. 2022). These applications typically use model-free policy optimization algorithms, such as PPO (Schulman et al. 2017), to learn control policies from high-dimensional sensory inputs. To achieve this, the control policies are often parameterized by deep neural networks. Policy optimization algorithms use massive rollout data to estimate the local gradient of the performance objective and then update the policy parameters in the direction of the estimated gradient. Thus, policy optimization algorithms are often on-policy and require large amounts of data to learn effective policies.

A promising alternative to model-free RL is model-based RL. In the context of robotics, this refers to algorithms that learn a dynamics model of the environment and use the model to plan actions or improve a policy. As model learning can be performed with off-policy data, these methods can significantly reduce the amount of real-world data required for training. The learned models are often used in two ways: (1) to generate synthetic data for policy optimization, and (2) to perform online planning.

Data generation for policy optimization: The first use case dates back to the early days of RL, when the Dyna approach was proposed (Sutton 1990). In this framework, a model of the environment is learned from real-world data and then used to generate synthetic data. Model-free RL algorithms are then applied on both real-world and synthetic data to optimize the policy. The approach originally showed effective at solving tabular RL problems, and has been extended to deep RL. The approach by Ha and Schmidhuber (2018) handles image inputs that are encoded to a latent space where they are subject to a latent dynamics model. The idea was continued in the Dreamer algorithms (Hafner et al. 2019a, 2020, 2025), which use learned latent dynamics models to generate synthetic data for policy training with actor-critic algorithms. The series of Dreamer algorithms has evolved over the years, and the latest version, DreamerV3 (Hafner et al. 2025), has shown the capability of learning complex behaviors in computer games and the possibility of handling different tasks with the same set of hyperparameters. There have been a few works that successfully applied the Dreamer algorithms to real-world robot control tasks, such as quadrupedal locomotion (Wu et al. 2023; Li et al. 2025b,a), solving a labyrinth game (Bi and D’Andrea 2024), and vision-based quadcopter control (Romero et al. 2025). In all of these works, advantages in sample efficiency have been reported. However, it was also noticed that running the model-free RL algorithms repeatedly with simulated data leads to the algorithm being the bottleneck of the training process instead of the data collection (Romero et al. 2025). Consequently, some existing works still perform model-based RL in simulation before transferring to the real world, implying they may still be affected by the sim-to-real gap (Li et al. 2025b; Romero et al. 2025).

Online planning via learned model: The second use-case takes advantage of the learned model for online planning. Some early works in this direction perform model predictive control with learned models to provide

expert samples for model-free RL finetuning (Nagabandi et al. 2018). A prominent example is the TD-MPC algorithm (Hansen et al. 2022, 2024), which combines model learning with online planning. In this approach, a latent-space dynamics model is learned from real-world data, along with a terminal value function. The learned models are subsequently used to perform online planning with a model predictive path integral search. This approach achieves great sample efficiency by leveraging off-policy data across multiple episodes for model learning. However, a significant computational overhead arises from the online sampling-based planning.

Learning-based Control for Complex Robot Systems

Although a wide range of successful applications of RL have been reported in the literature, many are limited to rigid-body systems with torque-controlled joints. In contrast, a wide range of real-world robotic systems are equipped with hydraulic or pneumatic actuators, or involve non-rigid objects as part of the robot's body or the environment. The control of these systems is often challenging, in particular due to the lack of simulators that match the accuracy and computational efficiency of their rigid-body counterparts. A number of methods have been proposed to address the lack of simulation tools. We present some representative examples in the context of hydraulic robots and soft robots, which are the platforms used to evaluate our approach.

The control of hydraulic actuators in robots is often considered in the context of the automation of heavy machinery. A number of works considered building a physics-based model of the hydraulic system, and then using nonlinear model-based control methods to develop controllers (Mattila et al. 2017). These methods, however, often face challenges when applied to real-world hydraulic systems, where the system dynamics cannot be fully understood. In this case, data-driven modeling has emerged as a promising alternative. Some early works use system identification methods to learn parameters in a physics-based model (Nurmi and Mattila 2017; Nurmi et al. 2018), which is then plugged into a model-based control framework. Later research used data-driven modeling to learn the complete dynamics model of the hydraulic system, and then used the model as a simulation environment for model-free RL (Egli and Hutter 2022). As the learned model contains the complex dynamics and coupling effects of the hydraulic system, the corresponding controller is able to achieve high-performance control on the modeled system. Subsequent works have combined physical modeling with learning-based methods to learn the residual dynamics of the hydraulic system, achieving both high performance and training efficiency (Lee et al. 2022). These RL-based methods, however, are limited by simulation environments. The trained policies only work well on the target system where the model is trained, and the performance degrades if the model is biased. This issue is partially addressed by the online adaptation approach proposed in (Nan and Hutter 2024), where the control policy is trained in simulation with a set of randomized system parameters and then adapted to the real-world system rapidly at the time of deployment. Real-world experiments show that

this approach is able to achieve high performance control on multiple hydraulic systems using online adaptation. The method, however, still requires a good understanding of the system model and careful selection of the parameters to be randomized, which limits its generalization to distinctly different systems.

Robots with soft structures share a lot of similar challenges in modeling and control. Modeling the dynamics of soft links with finite elements is accurate but slow for control purposes, while simplified models are often not sufficient to achieve performant control; thus, data-driven modeling is often recommended (Faure et al. 2012; Spinelli and Katzschnmann 2022). Previously, a number of works have used deep learning to predict the dynamics of soft robots for data synthesis and predictive control purposes (Chen et al. 2025; Sapai et al. 2023; Chen et al. 2024b). In (Li et al. 2022), a framework for an RL method for a pneumatically actuated soft robot is proposed. The approach combines pre-training in simulation and fine-tuning on real-world data in RL with Deep Deterministic Policy Gradient to efficiently learn an accurate controller for a three-chamber soft arm. The proposed method, however, still relies on an approximately accurate simulation model, and the real-world training is time-consuming. Researchers have also shown the possibility of performing optimization-based control with learned dynamics models (Bern et al. 2020). However, as pointed out by the authors, the approach is dependent on the accuracy of the learned model and does not have any capability for online refinement.

Online Learning for Control

Online learning provides a framework for sequential decision-making, where an agent iteratively improves its decisions based on feedback from the environment (Hazan 2019). The potential of integrating online learning principles into RL and control frameworks has recently emerged as a promising direction to achieve adaptive and robust control (Hazan and Singh 2025).

Recent work by Ma et al. (2024) draws connections between online learning and policy optimization. Extending the classic approach of iterative learning control (Hofer et al. 2019; Ma et al. 2022), they embed an approximate dynamics model into a stochastic, gradient-based online optimization loop. Their algorithm unifies first-order gradient descent and quasi-Newton updates using model-informed gradient estimates. The connection between modeling error and convergence is quantified, and sublinear regret is proven under general smoothness and bounded-error conditions. Experiments on a flexible beam, a quadruped robot, and a ping-pong robot demonstrate robust, real-time adaptation, even in the presence of noisy gradients. However, this approach focuses mainly on feedforward controller optimization and assumes access to a known model with bounded error.

Lin et al. (2024) addresses the limitation of requiring a known model by introducing a meta-framework that decouples the online policy optimizer (ALG) from the estimator of unknown dynamics (EST). They show that if ALG, when given perfect dynamics, satisfies certain contractivity and stability properties, then coupling ALG with EST only introduces bounded perturbations. The

cumulative effect of these perturbations scales with local estimation errors along the visited trajectory.

In this paper, we extend these strands by proposing a model-based RL algorithm with online learning inspirations. The algorithm includes an online model learning module to learn an explicit dynamics model, and uses its gradients to guide control policy updates. We provide a theoretical analysis to explain the effectiveness of the proposed online learning algorithm in nonlinear robot control problems, and demonstrate the effectiveness of the approach through real-world robot experiments.

Methodology

Problem formulation

We consider the problem of controlling an unknown dynamical system by minimizing a cost function over time. The system is described by a state $x_\tau \in \mathcal{X} \subseteq \mathbb{R}^n$ at each time step τ , and the control input is denoted by $u_\tau \in \mathcal{U} \subseteq \mathbb{R}^m$. We note that both \mathcal{X} and \mathcal{U} are bounded and convex. The system evolves according to the dynamics:

$$x_{\tau+1} = f(x_\tau, u_\tau), \quad (1)$$

where $f : \mathcal{X} \times \mathcal{U} \rightarrow \mathcal{X}$ is a function describing the system dynamics. We aim to find a control policy $\pi : \mathcal{X} \times \tilde{\mathcal{X}} \rightarrow \mathcal{U}$, where $\tilde{\mathcal{X}} \subseteq \mathbb{R}^p$ is also assumed to be bounded and convex, to minimize the expected cost in an episodic setting:

$$\begin{aligned}
 \min \quad & \mathbb{E} \left[\sum_{t=0}^{\infty} \sum_{\tau=0}^{H-1} c(x_{\tau}^{(t)}, u_{\tau}^{(t)}, \tilde{x}_{\tau}^{(t)}) \right] \\
 \text{s.t.} \quad & x_{\tau+1}^{(t)} = f(x_{\tau}^{(t)}, u_{\tau}^{(t)}) \\
 & u_{\tau}^{(t)} = \pi(x_{\tau}^{(t)}, \tilde{x}_{\tau}^{(t)}), \forall t \geq 0, \tau \geq 0
 \end{aligned} \tag{2}$$

where $x_\tau^{(t)}, \tau = 0, \dots, H-1$ is the state evolution according to (1) over episode t of length H . The cost function is denoted by $c : \mathcal{X} \times \mathcal{U} \rightarrow \mathbb{R}$, and may depend on the state, the control input, and an auxiliary random variable $\tilde{x}_\tau \in \tilde{\mathcal{X}}$, which represents reference trajectories or user commands. The reference trajectories $\tilde{x}_t = \left(\tilde{x}_0^{(t)}, \dots, \tilde{x}_{H-1}^{(t)} \right) \stackrel{\text{i.i.d.}}{\sim} \tilde{\mathcal{D}}$ are sampled at the beginning at each episode t , and $x_0^{(t)}$ is initialized according to $\tilde{x}_0^{(t)}$. By selecting the references with sufficient diversity, the learned policy can generalize well to arbitrarily long horizons.

Algorithm

To address (2) we propose a model-based RL algorithm that leverages the estimated system dynamics to optimize the control policy. We use a Neural Network (NN) f_θ to model the true dynamics function f , and the deterministic control policy is represented by another NN π_ϕ . The parameters $\theta \in \Theta \subseteq \mathbb{R}^{n_\theta}$ and $\phi \in \Phi \subseteq \mathbb{R}^{n_\phi}$ are optimized using stochastic gradient descent in an online manner. We also note that both Θ and Φ are bounded and convex. The proposed online model-based RL algorithm is outlined in Algorithm 1. Building on top of previous work on approximate gradient-based online learning, Algorithm 1 simultaneously learns a dynamics model online for calculating approximate policy gradients instead of assuming access to a known model. A

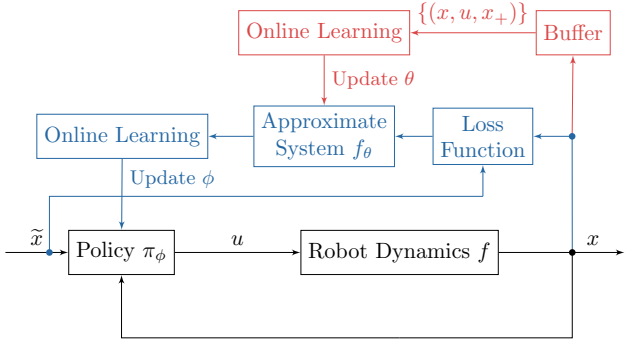


Figure 1. A diagram showing the workflow of the proposed online model-based RL algorithm. It involves online model learning and policy optimization at the same time. The red blocks highlight the process of model learning, and the blue components show the workflow of policy optimization.

diagram illustrating the workflow of the proposed algorithm is shown in Fig. 1.

Algorithm 1 Online Model-Based RL

```

1: Initialize parameters  $\theta, \phi$  and let  $\mathcal{D}_0 = \emptyset$ 
2: for  $t = 0, 1, \dots, T - 1$  do
3:   Sample reference  $\tilde{x}_{0:H}^{(t)} \in \tilde{\mathcal{D}}$ 
4:   Initialize state  $x_0 = \tilde{x}_0^{(t)}$ 
5:   for  $\tau = 0, 1, \dots, H$  do
6:     Compute control input  $u_\tau^{(t)} = \pi_\phi(x_\tau^{(t)}, \tilde{x}_\tau^{(t)})$ 
7:     Apply  $u_\tau^{(t)}$  and observe next state  $x_{\tau+1}^{(t)}$ 
8:   end for
9:   Extend the buffer:
10:   $\mathcal{D}_{t+1} \leftarrow \mathcal{D}_t \cup \{(x_\tau^{(t)}, u_\tau^{(t)}, x_{\tau+1}^{(t)})\}_{\tau=0}^{H-1}$ 
11:  Update dynamics model:
12:   $\theta_{t+1} \leftarrow \theta_t - \alpha_\theta \nabla_\theta \ell(\theta)$ 
     ▷ Using (3) evaluated on mini-batches from  $\mathcal{D}_{t+1}$ 
13:  Calculate controller loss:
14:   $g_t = \sum_{\tau=0}^{H-1} c(x_\tau^{(t)}, u_\tau^{(t)}, \tilde{x}_\tau^{(t)})$ 
15:  Calculate controller loss gradient according to (5)
16:  Estimate controller loss Hessian:
17:   $\Lambda_t = \widehat{\nabla}_\phi g_t \widehat{\nabla}_\phi g_t^\top + \alpha \frac{\partial u_{0:H}}{\partial \phi} \frac{\partial u_{0:H}}{\partial \phi}^\top + \epsilon \mathbf{I}$ 
18:  Policy update:
19:   $\phi_{t+1} \leftarrow \phi_t - \eta_t \Lambda_t^{-1} \widehat{\nabla}_\phi g_t$ 
20: end for

```

The proposed algorithm initializes both the dynamics model f_θ and the control policy π_ϕ randomly. In each episode t , we rollout the control policy for a fixed horizon H , and extend the buffer \mathcal{D} by the state-action-next-state tuples. Similar to many existing model-based RL algorithms, we approximate the dynamics model by minimizing the mean squared error for single-step prediction:

$$\ell(\theta) = \mathbb{E}_{(x, u, x^+) \sim \mathcal{D}} \|f_\theta(x, u) - x^+\|^2. \quad (3)$$

In practice, we sample a mini-batch $\{(x_i, u_i, x_{i+1})\}_i$ from the buffer \mathcal{D}_{t+1} at episode t .

After updating the model, we compute an analytical policy gradient on the policy parameter ϕ using the closed-loop gradient. Recall that the cost function for the trajectory

rollout in episode t is defined as:

$$g\left(\phi^{(t)}; \tilde{\mathbf{x}}^{(t)}\right) = \sum_{k=0}^{H-1} c(x_\tau^{(t)}, u_\tau^{(t)}, \tilde{x}_\tau^{(t)}) \quad (4)$$

$$u_\tau^{(t)} = \pi_{\phi^{(t)}}(x_\tau^{(t)}, \tilde{x}_\tau^{(t)}), \quad x_{\tau+1}^{(t)} = f(x_\tau^{(t)}, u_\tau^{(t)}).$$

While the true dynamics model f is unknown, we use the learned dynamics model f_θ instead in the calculation. We first compute block Jacobian matrices $A_t \in \mathbb{R}^{nH \times nH}$, $B_t \in \mathbb{R}^{nH \times mH}$, and $K_t \in \mathbb{R}^{mH \times nH}$, each composed of $H \times H$ blocks:

$$[A_t]_{ij} = \begin{cases} \frac{\partial f_\theta(x_j^{(t)}, u_j^{(t)})}{\partial x_j^{(t)}}, & i = j + 1, \\ \mathbf{0}, & \text{otherwise,} \end{cases}$$

$$[B_t]_{ij} = \begin{cases} \frac{\partial f_\theta(x_j^{(t)}, u_j^{(t)})}{\partial u_j^{(t)}}, & i = j + 1, \\ \mathbf{0}, & \text{otherwise,} \end{cases}$$

$$[K_t]_{ij} = \begin{cases} \frac{\partial \pi_\phi(x_j^{(t)}, \tilde{x}_j^{(t)})}{\partial x_j^{(t)}}, & i = j, \\ \mathbf{0}, & \text{otherwise,} \end{cases}$$

for $i, j \in \{0, \dots, H-1\}$. Denote $\mathbf{x}_t = \text{vec}(x_0^{(t)}, \dots, x_{H-1}^{(t)})$ and $\mathbf{u}_t = \text{vec}(u_0^{(t)}, \dots, u_{H-1}^{(t)})$ as the concatenated state and control trajectories of the rollout in episode t . Then, we estimate the policy gradient as:

$$\widehat{\nabla}_\phi g(\phi_t; \tilde{\mathbf{x}}_t) = \frac{\partial g(\phi_t; \tilde{\mathbf{x}}_t)}{\partial \mathbf{x}_t} (\mathbf{I} - (A_t + B_t K_t))^{-1} B_t \frac{\partial \mathbf{u}_t}{\partial \phi}, \quad (5)$$

where $\widehat{\nabla}_\phi g(\phi_t; \tilde{\mathbf{x}}_t)$ captures the closed-loop sensitivity of the cost $g(\phi_t; \tilde{\mathbf{x}}_t)$ with respect to the policy parameters ϕ_t , taking into account the feedback effects through the system dynamics and the control policy. As $A_t + B_t K_t$ is only non-zero on the first upper diagonal blocks, the matrix inversion in (5) essentially unrolls the closed-loop dynamics over time.

The calculation in (5) is different from common implementations of back-propagation through time (BPTT) algorithm, which typically uses differentiable dynamics for forward simulation and computes the gradients using a backward pass through the computation graph (Zhang et al. 2025). This is not possible in our case, as the real dynamics are unknown. Yet the Jacobian of the learned dynamics model f_θ can be used to evaluate an approximate gradient along the actual rollout trajectory. While the learned model may be inexact, i.e., $f_\theta(x_\tau, u_\tau) \neq x_{\tau+1}$, the input-output Jacobians of f_θ can still provide useful information about the local dynamics along the true trajectory. With this technique, we avoid rolling out the learned model to collect trajectories, which would be affected by compounding errors, and gain significant computational efficiency as we can use first-order optimization methods on real trajectories.

The policy optimization in Alg. 1 uses a pre-conditioned online gradient descent algorithm:

$$\phi_{t+1} = \phi_t - \eta_t \Lambda_t^{-1} \widehat{\nabla}_\phi g(\phi_t; \tilde{\mathbf{x}}_t), \quad (6)$$

where η_t is the learning rate, and the pre-conditioner Λ_t is defined as:

$$\widehat{\nabla}_\phi g(\phi_t; \tilde{\mathbf{x}}_t) \widehat{\nabla}_\phi g(\phi_t; \tilde{\mathbf{x}}_t)^\top + \alpha \frac{\partial u_{0:H}}{\partial \phi} \frac{\partial u_{0:H}}{\partial \phi}^\top + \epsilon \mathbf{I}. \quad (7)$$

The policy optimization step (6) solves an optimization problem with linearized objective and Λ_t -norm regularization. As π_ϕ and f_θ are both highly nonlinear functions, the estimated gradient $\widehat{\nabla}_\phi g(\phi_t; \tilde{\mathbf{x}}_t)$ is likely to be inaccurate once the policy changes significantly, thus the regularization is necessary to stabilize the learning algorithm. The three terms in (7), controlled by the hyperparameters α and ϵ , restrict policy parameter updates that cause significant changes in the objective function, control actions, and policy parameters, respectively. A similar regularization has been used in (Ma et al. 2024), where it was interpreted as a trust region approach to prevent the policy from changing too much in each episode.

Theoretical Analysis

We analyze the proposed algorithm from an online learning perspective and justify that the control policy converges under necessary assumptions and appropriate selection of the hyperparameters. Algorithm 1 can be viewed as simultaneously solving two interleaved online learning problems: the online model learning and the online policy learning. Specifically, the online policy learning relies on the learned dynamics model to compute an approximate policy gradient, while the online model learning is affected by policy updates because updated policies induce shifting data distributions in the buffer \mathcal{D} . While formally analyzing the joint dynamics of the two learning problems is difficult, we separately analyze the two problems under necessary assumptions. Each problem is analyzed as a special case of online learning, and in the end, we discuss how joint convergence can be achieved for Algorithm 1.

Online Policy Learning The online policy learning can be viewed as an online optimization problem with an inexact loss gradient. We let $\phi^* = \arg \min_{\phi \in \Phi} \mathbb{E}_{\tilde{\mathbf{x}} \sim \tilde{\mathcal{D}}} [g(\phi; \tilde{\mathbf{x}})]$ and define the expected regret for the policy learning as:

$$\mathbb{E}[\mathbf{R}_T] \doteq \mathbb{E} \left[\sum_{t=1}^T g(\phi_t; \tilde{\mathbf{x}}_t) - g(\phi^*; \tilde{\mathbf{x}}_t) \right]. \quad (8)$$

Furthermore, we assume that the cost function g is L_g -Lipschitz continuous and β_g -smooth for any $\tilde{\mathbf{x}} \in \tilde{\mathcal{X}}$ and $\phi, \phi' \in \Phi$. Then we have

$$g(\phi'; \tilde{\mathbf{x}}) \leq g(\phi; \tilde{\mathbf{x}}) + \langle \nabla_\phi g(\phi; \tilde{\mathbf{x}}), \phi' - \phi \rangle + \frac{\beta_g}{2} \|\phi' - \phi\|^2.$$

Plugging in the policy update rule (6), we get,

$$g(\phi_{t+1}; \tilde{\mathbf{x}}) \leq g(\phi_t; \tilde{\mathbf{x}}) - \eta_t \langle \nabla_\phi g(\phi_t; \tilde{\mathbf{x}}), \Lambda_t^{-1} \widehat{\nabla}_\phi g(\phi_t; \tilde{\mathbf{x}}) \rangle + \frac{\beta_g \eta_t^2}{2} \|\Lambda_t^{-1} \widehat{\nabla}_\phi g(\phi_t; \tilde{\mathbf{x}})\|^2.$$

We denote the gap between the true gradient and the approximate gradient as $\delta_t \doteq \widehat{\nabla}_\phi g(\phi_t; \tilde{\mathbf{x}}) - \nabla_\phi g(\phi_t; \tilde{\mathbf{x}})$, and we can rewrite the above equation as

$$g(\phi_{t+1}; \tilde{\mathbf{x}}) \leq g(\phi_t; \tilde{\mathbf{x}}) - \eta_t \langle \nabla_\phi g(\phi_t; \tilde{\mathbf{x}}), \Lambda_t^{-1} \nabla_\phi g(\phi_t; \tilde{\mathbf{x}}) \rangle - \eta_t \langle \nabla_\phi g(\phi_t; \tilde{\mathbf{x}}), \Lambda_t^{-1} \delta_t \rangle + \frac{\beta_g \eta_t^2}{2} \|\Lambda_t^{-1} \widehat{\nabla}_\phi g(\phi_t; \tilde{\mathbf{x}})\|^2. \quad (9)$$

By the definition (7), Λ_t is a positive definite matrix due to the sum of two outer products and a scaled identity matrix. Thus, the eigenvalues of Λ_t^{-1} are well-defined and bounded as long as $\widehat{\nabla}_\phi g(\phi_t; \tilde{x})$ and $\partial u_{0:H}/\partial \phi$ have bounded norms. We assume this property holds, and the eigenvalues of Λ_t are bounded by

$$0 < m \leq \lambda_{\min}(\Lambda_t) \leq \lambda_{\max}(\Lambda_t) \leq M,$$

for all $t \geq 0$. Therefore, we can bound the first term in (9) as follows

$$\langle \nabla_\phi g(\phi_t; \tilde{x}), \Lambda_t^{-1} \nabla_\phi g(\phi_t; \tilde{x}) \rangle \geq \frac{1}{M} \|\nabla_\phi g(\phi_t; \tilde{x})\|^2.$$

The second term in (9) can be bounded using the Cauchy-Schwarz inequality:

$$\begin{aligned} & |\langle \nabla_\phi g(\phi_t; \tilde{x}), \Lambda_t^{-1} \delta_t \rangle| \\ & \leq \|\nabla_\phi g(\phi_t; \tilde{x})\| \cdot \|\Lambda_t^{-1} \delta_t\| \leq \frac{L_g}{m} \|\delta_t\|. \end{aligned}$$

The last term in (9) can be bounded by the Lipschitz property of g :

$$\|\Lambda_t^{-1} \widehat{\nabla}_\phi g(\phi_t; \tilde{x})\|^2 \leq \frac{1}{m^2} \|\widehat{\nabla}_\phi g(\phi_t; \tilde{x})\|^2 \leq \frac{L_g^2}{m^2}.$$

Putting the bounds together, we have

$$\begin{aligned} g(\phi_{t+1}; \tilde{x}) & \leq g(\phi_t; \tilde{x}) - \frac{\eta_t}{M} \|\nabla_\phi g(\phi_t; \tilde{x})\|^2 \\ & \quad + \frac{\eta_t L_g}{m} \|\delta_t\| + \frac{\beta_g \eta_t^2 L_g^2}{2m^2}. \end{aligned} \quad (10)$$

We note that (10) provides a bound for the loss change in one update of the policy parameter. While the term $-\|\nabla_\phi g(\phi_t; \tilde{x})\|^2$ is always non-positive, the gradient estimation error δ_t needs to be controlled to ensure the convergence. We provide one method to derive the requirement on δ_t by assuming a Polyak-Łojasiewicz (PL) condition on the loss function g for any $\tilde{x} \in \mathcal{D}$ and $\phi \in \Phi$

$$\|\nabla_\phi g(\phi; \tilde{x})\|^2 \geq 2\mu(g(\phi; \tilde{x}) - g(\phi^*; \tilde{x})), \quad \mu > 0.$$

The PL assumption relates the gradient norm to the function value gap compared to the optimal parameters. In our case, $g(\phi_t; \tilde{x}) - g(\phi^*; \tilde{x})$ is exactly the regret in episode t . Therefore we could rewrite (10) in the following form

$$\begin{aligned} & g(\phi_{t+1}; \tilde{x}) - g(\phi^*; \tilde{x}) \\ & \leq \left(1 - \frac{2\mu\eta_t}{M}\right) (g(\phi_t; \tilde{x}) - g(\phi^*; \tilde{x})) \\ & \quad + \frac{\eta_t L_g}{m} \|\delta_t\| + \frac{\beta_g \eta_t^2 L_g^2}{2m^2}. \end{aligned} \quad (11)$$

We let $G(\phi) \doteq \mathbb{E}[g(\phi; \tilde{x})]$ and take the expectation on both sides to obtain a recursive inequality for the expected regret:

$$\begin{aligned} & G(\phi_{t+1}) - G(\phi^*) \\ & \leq \left(1 - \frac{2\mu\eta_t}{M}\right) (G(\phi_t) - G(\phi^*)) \\ & \quad + \mathbb{E}\left[\frac{\eta_t L_g}{m} \|\delta_t\|\right] + \frac{\beta_g \eta_t^2 L_g^2}{2m^2}. \end{aligned} \quad (12)$$

This recursion suggests that the expected regret in each episode has a decreasing term driven by the online gradient descent as long as $\eta_t < M/2\mu$. However, an error term appears due to the inexact gradient, in addition to the term from higher-order residuals. One can see that a necessary condition for the learned policy to achieve optimal performance is to have the gradient estimation error δ_t converge to 0.

To derive a sufficient condition on δ_t , we unroll the recursion in (12). Let $\eta_t = \eta$ for all t with $1 - \frac{2\mu\eta}{M} \in (0, 1)$, and assuming $G(\phi_0) - G(\phi^*) \leq D$ for some constant D , the previous expression can be simplified to

$$\begin{aligned} G(\phi_t) - G(\phi^*) & \leq \left(1 - \frac{2\mu\eta}{M}\right)^t D \\ & \quad + \frac{\eta L_g}{m} \mathbb{E}\left[\sum_{\tau=0}^{t-1} \left(1 - \frac{2\mu\eta}{M}\right)^{t-\tau} \|\delta_\tau\|\right] \\ & \quad + \frac{\beta_g \eta^2 L_g^2}{2m^2} \sum_{\tau=0}^{t-1} \left(1 - \frac{2\mu\eta}{M}\right)^{t-\tau}. \end{aligned}$$

Next, we sum over $t = 1, 2, \dots, T$, we have

$$\begin{aligned} \mathbb{E}[R_T] & = \mathbb{E}\left[\sum_{t=1}^T g(\phi_t) - \sum_{t=1}^T g(\phi^*)\right] \\ & \leq \underbrace{\sum_{t=1}^T \left(1 - \frac{2\mu\eta}{M}\right)^t D}_{(A)} \\ & \quad + \underbrace{\frac{\eta L_g}{m} \sum_{t=1}^T \mathbb{E}\left[\sum_{\tau=0}^{t-1} \left(1 - \frac{2\mu\eta}{M}\right)^{t-\tau} \|\delta_\tau\|\right]}_{(B)} \\ & \quad + \underbrace{\frac{\beta_g \eta^2 L_g^2}{2m^2} \sum_{t=1}^T \sum_{\tau=0}^{t-1} \left(1 - \frac{2\mu\eta}{M}\right)^{t-\tau}}_{(C)} \end{aligned}$$

From the sum of a geometric series, for large enough T , we have

$$(A) \leq D \cdot \frac{M}{2\mu\eta} = \mathcal{O}(\eta^{-1}).$$

We rearrange the sums in (B),

$$\begin{aligned} (B) & = \frac{\eta L_g}{m} \mathbb{E}\left[\sum_{t=1}^T \sum_{\tau=0}^{t-1} \left(1 - \frac{2\mu\eta}{M}\right)^{t-\tau} \|\delta_\tau\|\right] \\ & \leq \frac{\eta L_g}{m} \mathbb{E}\left[\sum_{\tau=0}^{T-1} \sum_{t=\tau+1}^T \left(1 - \frac{2\mu\eta}{M}\right)^{t-\tau} \|\delta_\tau\|\right] \\ & \leq \frac{\eta L_g}{m} \frac{M}{2\mu\eta} \left(1 - \left(1 - \frac{2\mu\eta}{M}\right)^T\right) \mathbb{E}\left[\sum_{\tau=0}^{T-1} \|\delta_\tau\|\right]. \end{aligned}$$

By Cauchy-Schwarz and Jensen's inequality, the last term

$$\mathbb{E}\left[\sum_{\tau=0}^{T-1} \|\delta_\tau\|\right] \leq \sqrt{T \cdot \sum_{\tau=0}^{T-1} \|\delta_\tau\|^2} \leq \sqrt{T \cdot \mathbb{E}\left[\sum_{\tau=0}^{T-1} \|\delta_\tau\|^2\right]},$$

and the bound on (B) simplifies to

$$(B) \leq C \cdot \sqrt{T} \sqrt{\mathbb{E} \left[\sum_{\tau=0}^{T-1} \|\delta_\tau\|^2 \right]}, \quad C = \frac{\eta L_g M}{2\mu m}.$$

Finally, for the term (C), we have

$$(C) \leq \frac{\beta_g \eta^2 L_g^2}{2m^2} \frac{MT}{2\mu\eta} = \mathcal{O}(\eta T).$$

Combining all the terms, we have

$$\mathbb{E}[\mathbf{R}_T] \leq \mathcal{O}(\eta^{-1}) + \mathcal{O}(\eta T) + C \cdot \sqrt{T \mathbb{E} \left[\sum_{\tau=0}^{T-1} \|\delta_\tau\|^2 \right]}. \quad (13)$$

The final regret bound (13) consists of the standard terms in online optimization, and an additional term that depends on the cumulative gradient prediction error $\mathbb{E} \left[\sum_{\tau=0}^{T-1} \|\delta_\tau\|^2 \right]$.

The first two terms can be balanced to \sqrt{T} by setting $\eta = \mathcal{O}(T^{-1/2})$, while the last term depends on the quality of the learned dynamics model. Some special cases of (13) have been studied in the literature. If the exact model is available (i.e., $\delta_t = 0$), the regret bound reduces to $\mathcal{O}(\sqrt{T})$, recovering the standard online convex optimization result. If one applies the proposed algorithm with a prebuilt dynamics model that guarantees gradient prediction error bounded by a constant $\|\delta_t\| \leq \delta$, then the last term is $\mathcal{O}(T)$, leading to a linear regret. If additional assumptions on the direction of predicted gradient are made, one can still achieve sublinear regret by controlling the cross-product term in (9). This case has been thoroughly studied in (Ma et al. 2024).

More generally, (13) suggests a sufficient condition for policy learning to achieve sublinear regret is to have $\mathbb{E} \left[\sum_{\tau=0}^{T-1} \|\delta_\tau\|^2 \right] = o(T)$. In Algorithm 1, this requires the online model learning to converge sufficiently fast.

Online Model Learning The previous derivation (13) shows that the regret of the policy learning depends on the expected cumulative gradient prediction error. Before proceeding to analyze the online model learning problem itself, we first clarify the relationship between the model prediction error and the gradient prediction error.

As we do not have access to the true dynamics model or its gradient, the model learning part in Algorithm 1 is performed to minimize the one-step prediction error defined in (3). We justify that a model learned to accurately perform one-step prediction also has a small Jacobian prediction error under appropriate assumptions. Many physical dynamical systems, in particular those considered in robotics, show continuity and smoothness, i.e., small changes in the state and control inputs lead to small changes in the next state. Therefore, if a learned dynamics model accurately predicts the one-step transitions on a certain distribution of state-action pairs, it is likely that the learned model's Jacobian is also close to the true dynamics' Jacobian. This intuition requires the distribution of the data used for model learning to be sufficiently rich, e.g., it must have sufficient probability density in the neighborhood of the trajectory for which we compute the policy gradient. A formal analysis of this property from the perspective of measure theory can be

found in (Lin et al. 2024). In many robotic applications, the noise in system dynamics and measurement naturally injects randomness into the collected data. Additionally, the use of randomly initialized control policies and sampled commands further enriches the data distribution. Therefore, we assume that the data distribution used for model learning is sufficiently rich to support using the model Jacobian, although the model is only trained to minimize prediction error.

The Jacobian of the learned model is used to compute the policy gradient using (5). Therefore, the policy gradient prediction error δ_t depends not only on the model Jacobian error, but also on the sensitivity of the closed-loop system formed by the dynamics and the control policy. To avoid the error getting amplified by the $(\mathbf{I} - (A_t + B_t K_t))^{-1}$ term in (5), the closed-loop system must be stable. This property can be assumed to hold in the initial phase for randomly initialized control policies and dissipative dynamics. A discounting factor on the $A_t + B_t K_t$ term could also be used to further ensure computational stability.

The online model learning in Alg. 1 is performed similarly to standard online stochastic gradient descent. However, unlike common online learning settings where the data is i.i.d. sampled from a constant distribution, the data distribution in our case is affected by the current control policy. Specifically, the online model learning is always performed on the buffer \mathcal{D}_t containing data collected from episode 1 to t , and only used to compute the policy gradient on the current episode trajectory. To analyze the model learning convergence with this distribution shift, we denote the distribution of the data collected in episode t as ν_t , and the distribution of the data in the buffer \mathcal{D}_t . The distribution ν_t can be slowly changing as the policy is updated in each episode. We use $\Delta_t \doteq \|\nu_t - \nu_{t-1}\|_{\text{TV}}$ to denote the Total Variation (TV) distance between ν_t and ν_{t-1} . We impose the assumptions that:

- f, f_θ , are Lipschitz continuous and smooth functions;
- \mathcal{X} and \mathcal{U} are bounded compact sets;
- the loss function in (3) satisfies a PL condition.

The expected model learning regret is defined as

$$\mathbb{E}[\bar{\mathbf{R}}_T] = \sum_{t=1}^T \mathbb{E}_{z \sim \nu_t} \ell(\theta_t; z) - \sum_{t=1}^T \mathbb{E}_{z \sim \nu_t} \ell(\theta_t^\diamond; z), \quad (14)$$

where $\theta_t^\diamond = \arg \min_\theta \mathbb{E}_{z \sim \nu_t} \ell(\theta; z)$. One can show that (14) is bounded by the learning rate α and Δ_t , $t = 1, 2, \dots, T$ as

$$\begin{aligned} \mathbb{E}[\bar{\mathbf{R}}_T] &\leq C_0 \sum_{t=1}^T \frac{1}{t} \sum_{i=2}^t (i-1) \Delta_i \\ &\quad + \frac{C_1}{\alpha} 4K \sum_{t=1}^T \Delta_t + C_2 \alpha T + \frac{C_3}{\alpha}, \end{aligned} \quad (15)$$

where C_0, C_1, C_2, C_3 are constants. Similar to the analysis for policy learning in (8)-(13), one can decompose the online gradient descent steps and isolate the disturbance caused by the shifting data distribution. The detailed derivation is left to the Appendix.

The bound (15) suggests the influence of the distribution shift Δ_t on the online model learning process is two-fold. The first term, originally from (A) and (C), measures

the performance gap for training with the buffered data but only performing predictions on the current episode data. The second term, originally from (B), is due to the shifting distribution of the training data. As the training data distribution is the uniform mixture of all past episode data distributions, the distribution shift Δ_t is discounted by a factor of $1/t$, suggesting a single episode of data having a different distribution from the rest has a diminishing effect on the model learning process as more data is collected.

One can also see that when the data distribution across episodes is stationary (i.e., $\Delta_t = 0$), the regret bound reduces to $\mathcal{O}(\sqrt{T})$ by taking the optimal $\alpha \propto 1/\sqrt{T}$, which is consistent with the standard online gradient descent result for convex problems. In case the distribution shift is bounded by a constant, i.e., $\Delta_t \leq D$, the bound becomes $\mathcal{O}(T) + \mathcal{O}(T/\alpha) + \mathcal{O}(\alpha T) + \mathcal{O}(1/\alpha)$, and sublinear regret cannot be achieved.

Summary The analysis above has separately considered the online learning problems for model learning and policy learning. In practice, the two problems are coupled through the gradient prediction error δ_t and the data distribution shift Δ_t , which creates difficulties for formal analysis.

In Algorithm 1, a strong regularization on the policy update is used to ensure small changes between two consecutive policies. This reduces the distribution shift Δ_t caused by the changing policy, and the model learning can view the data distribution as approximately stationary after an initial burn-in period to enrich the data buffer. After this, the model learning problem becomes near-stationary and achieves fast convergence. Literatures (Bubeck 2015) have shown that for strongly convex or PL-satisfying problems, the convergence rate of $1/t$ could be achieved with appropriate learning rate selection. Practically, we could also use adaptive gradient methods such as Adam (Kingma and Ba 2015) to accelerate the convergence. Assuming this faster convergence rate is achieved for δ_t , the remainder term in (13) can be absorbed by the \sqrt{T} term. This lead to an effect of time-scale separation between the model learning and policy learning processes. Similar technique is also used in adaptive control (Liberzon 2016).

Remarks We analyze the algorithm by studying two isolated online learning problems: the online policy optimization with learned model, and the online model learning with shifting data distribution. Several assumptions about the controlled system and the learning process. Most assumptions on bounded state and action spaces, Lipschitz continuity, and smoothness of the dynamics function are common to many robotic systems. While the PL condition is a strong assumption we made in order to show the convergence of the online optimization, recent success in deep learning suggests that high-dimensional non-convex problems can still be optimized effectively. The effectiveness of the proposed algorithm is also verified on different robotic systems in our experiments.

The presented theoretical analysis is not limited to the proposed algorithm. The model learning convergence analysis seamlessly extends to other model-based RL algorithms, as many of them have the same setting of data accumulation in a buffer and Stochastic Gradient Descent (SGD) updates per episode. The main difference is that the

policy difference between two consecutive episodes is not necessarily small, which is more likely to cause instabilities. In addition, the relationship between the model prediction regret bound and control policy regret bound in those algorithms needs to be analyzed separately.

The analysis for the policy training problem is closely related to the use of differentiable models to optimize the control policy. As a widely used technique in a number of algorithms from iterative learning control (Pierallini et al. 2025; Ma et al. 2022) to RL in differentiable simulation (Song et al. 2024; Zhang et al. 2025), it has been shown that even inaccurate gradient information from a surrogate model can be used to effectively optimize control policies. Previous analyses have shown that the convergence of approximate gradient-based algorithms is only guaranteed if the model always predicts the correct direction of the gradient (Ma et al. 2024). While models satisfying this guarantee may be hard to obtain for robotic systems with multiphysical dynamics, our analysis shows it is possible to mitigate this requirement with online model learning. In particular, from the analysis of policy learning, we notice that for any model learning process with square-summable gradient prediction error, the policy optimization process can achieve a regret bound related to the model error. This suggests that the sublinear regret bound for control policy learning can be achieved by combining the proposed online policy learning with any model learning process that achieves sublinear regret bounds.

Online optimization of multiple models in the same pipeline, combined with changing objectives and data distributions, is also commonly seen in many model-free RL algorithms, such as the Q-function and policy in DDPG (Lillicrap et al. 2015), and the actor and critic in SAC or PPO (Haarnoja et al. 2018; Schulman et al. 2017). A similar analysis can be applied to these approaches, potentially helping to interpret the instabilities and justify the necessity for regularization.

Experiment

We evaluate the proposed algorithm on two real-world robotic platforms: a hydraulic robot excavator and a cable-driven soft robot arm. Both systems present distinct challenges in control, as their actuation dynamics are highly nonlinear, difficult to model, and exhibit significant heterogeneity—each unit differs and requires separate modeling. We applied the proposed online model-based RL approach to all of them and successfully learned control policies that adapt to the system dynamics and achieve high control accuracy.

HEAP

HEAP is a 12.5-ton hydraulic excavator developed for autonomous construction purposes (Jud et al. 2021). It is equipped with computer-controlled proportional valves for each hydraulic actuator and high-precision proprioceptive sensors, enabling precise state estimation and automatic control. Accurate control of the hydraulic-actuated arm of HEAP is crucial for tasks such as grading, digging, and loading. While previous works to achieve this task always rely on some form of modeling, either through manual



Figure 2. HEAP, the autonomous excavator used in the experiments.

calibration and system identification (Jud et al. 2021) or data-driven modeling (Egli and Hutter 2022), we apply the proposed online model-based RL algorithm to obtain a control policy directly in one step.

The goal of the task is to control the excavator arm to follow a desired trajectory, which is defined by a sequence of target positions in the Cartesian space associated with time stamps. The control policy is trained to minimize the tracking error, defined as the Euclidean distance between the current position and the target position at this time step. The target trajectories are generated as polynomial functions with continuous first and second derivatives, ensuring smooth transitions. Each trajectory lasts for 5 seconds, and each episode of training consists of 10 such trajectories. As the system exhibits significant delay, we provide as input to the control policy not only the current position and velocity of the excavator arm joints but also a lookahead window of the target trajectory, along with the previous current commands. The control policy is trained to predict a current command for each valve, which is then applied to the system. The model is trained to predict the velocity of the arm at the next time step, which is then used to compute the next position. Both the model and the control policy are represented by neural networks with two hidden layers. Although both the model and the control policy are trained with online SGD in the analysis, we observe that using the Adam optimizer (Kingma and Ba 2015) for model learning significantly improves the convergence speed. Therefore, we use Adam for model learning and SGD for control policy learning in the experiments.

Simulation We first evaluate the proposed algorithm in a simulation environment of HEAP. The simulation environment is built with the model created by Egli and Hutter (2022). Trained with approximately 100 min of data, the simulation uses a neural network to model the complex dynamics of HEAP’s arm.

Deploying the proposed online model-based RL algorithm in the simulation environment results in convergence of episodic loss in both model learning and control policy learning, as shown in Figure 3.

The constant rate decreasing period in the log-scale loss plots indicates a power-law convergence behavior after the initial burn-in phase. The burn-in phase is most likely caused by the limited data buffer size in the first few episodes,

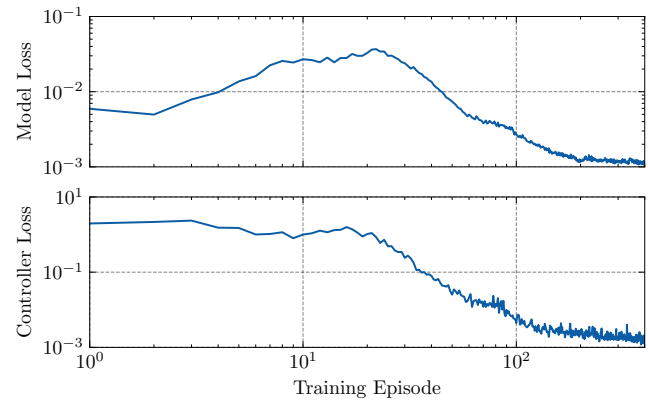


Figure 3. Convergence of the online model-based RL algorithm in HEAP simulation. The plots show the average loss in model learning and control policy learning over 10 runs. The shaded area represents the standard deviation. Both mean and standard deviation are computed on a log scale.

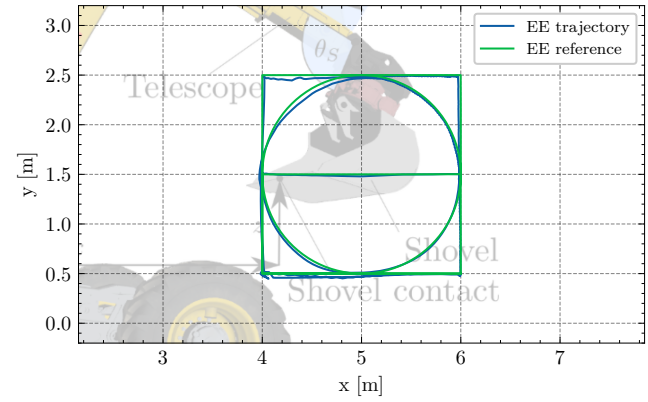


Figure 4. Evaluation of the control policy learned in simulation after 200 episodes. The plots show the tracking error of the control policy on a set of unseen reference trajectories that consists of straight lines and circles.

which results in a high variance in model learning and non-improving control policy performance. After the first 10 episodes, a stable learning process is established, and the model and control policy losses decrease at a constant rate. Measuring the slope of the policy loss in this segment, we estimate the convergence rate approximately $\ell_t \propto t^{-4}$. After 200 episodes, the learning slows down significantly, and the loss reaches a plateau. We suspect this is due to the complexity of the task limiting the achievable performance.

The controller performance of the online learning policy, after 200 training episodes, is evaluated on a set of unseen reference trajectories, and the results are shown in Figure 4. The control policy achieves a mean tracking error of 2.5 cm, with only 2.78 h of training data experienced in simulation. In comparison, model-free policy gradient methods such as PPO, as implemented by Egli and Hutter (2022) uses equivalence of 1.67 h of simulated experience per episode, and takes 8000 episodes to converge. This drastic reduction in training time and data usage is a key advantage of the proposed online model-based RL algorithm and allows us to directly deploy the online learning algorithm on the real robot.

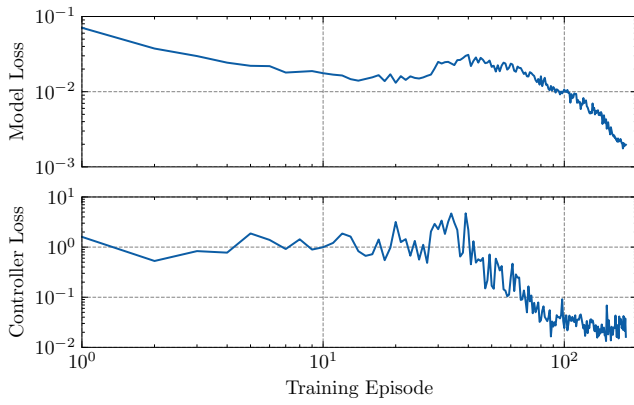


Figure 5. Real-world deployment results on the HEAP excavator. The plots show convergence, evaluation metrics, and adaptation to payload changes.

Real-World Deployment With the successful application of the proposed online model-based RL algorithm in simulation, we deploy the algorithm on the real HEAP excavator. We initialize the model and control policy randomly as done in the simulation experiment, and run the online learning algorithm for 180 episodes. This corresponds to 2.5 h of real-world training data. The total experiment time is approximately 3 h with the algorithm running on a desktop workstation*.

The losses of the training process are shown in Figure 5. We also record the performance of the control policy over training episodes at different times and plot the results in Figure 6.

The performance of the control policy reaches a mean tracking error of 2.7 cm following random spline trajectories after 180 episodes. A detailed comparison of the accuracy with previous approaches of sim-to-real transfer and sim-to-real with online adaptation (Egli and Hutter 2022; Nan and Hutter 2024) is shown in Table 1. The table shows several metrics, including the average velocity v^{avg} , maximum velocity v^{max} , average positional tracking error $|e_p|^{\text{avg}}$, maximum positional tracking error $|e_p|^{\text{max}}$, and the normalized performance indicator $\rho = |e_p|^{\text{max}}/v^{\text{max}}$ introduced in previous papers by Mattila et al. (2017).

The online learning approach achieves significantly higher velocity with similar or better normalized accuracy compared to previous approaches. Table 1 lists the highest velocity performance reported by Egli and Hutter (2022) and reproduced results of Nan and Hutter (2024) at higher speed. Yet, the previous approaches cannot achieve similar accuracy even at half the achieved speed. Specifically, ρ reduced by 30% when the maximum velocity more than doubled compared to Egli and Hutter (2022), which uses a data-driven model for the particular machine to train an RL controller. The reason is that the previous approach relies on the quality of the learned model, which heavily degrades at high speeds due to the limited training data. While Nan and Hutter (2024) achieves higher velocity with its randomized pre-training and online adaptation approach, the accuracy is not comparable at high speed. This is likely due to the fact that the randomized pre-training relies a simplified model of the hydraulic excavator, which has higher discrepancy with the real system because of the coupling between

joints and load-dependent dynamics. As the proposed online learning algorithm directly learns from real-world data, these limitations are avoided, and the algorithm is able to achieve better accuracy at high speed.

Table 1. Trajectory tracking performance and comparison with previous approach. The data of the baseline methods is taken from Egli and Hutter (2022) and by reproducing the result in Nan and Hutter (2024) at a higher speed.

Metric	Online learning	(N&H24)	(E&H22)
v^{avg} [cm/s]	52.3	37.5	20
v^{max} [cm/s]	129.3	60	52.5
$ e_p ^{\text{avg}}$ [cm]	4.5	8.56	2.8
$ e_p ^{\text{max}}$ [cm]	12.4	16.2	6.7
ρ [s]	0.09	0.27	0.13

The robustness of the online learning algorithm is also demonstrated by its ability to adapt to shifting dynamics. We verify this by changing the payload of the excavator arm, taking the gripper end effector, and switching to boulders of different weights in the gripper. During this process, the online learning algorithm learns to perform the same trajectory tracking task without information about the payload change. The online learning algorithm is able to adapt to the disturbances and quickly learns to control the arm with the new payload, despite the fact that the underlying dynamics model has changed. The loss plots with payload changes during online learning are shown in Figure 7. It can be seen that, despite having significantly higher randomness in the data, the model and control policy losses still decrease over time. After the first 100 episodes, we observe that the controller loss increases significantly when the payload changes, but quickly recovers to a lower level after a few episodes. One example of the payload switch at episode 157 is shown in Figure 8. The plot shows the tracking performance at episode 156 when the algorithm has been trained with a small rock payload, episode 157 right after switching to a large rock payload, and episode 162 after a few episodes of adaptation. After the payload switch, the tracking error immediately doubles, but quickly reduces back to a similar level as before after five episodes of training adaptation. This shows that the online learning algorithm is able to adapt to the new payload conditions, although the algorithm was not explicitly designed to handle such disturbances.

Soft Robot Arm

The online learning algorithm is further evaluated on a cable-driven soft robot arm shown in Figure 9. The hardware platform, designed by Guan et al. (2023), consists of three helicoid segments, each driven by three cables connected to a spool driven by a motor in the base. As the helicoid segment shall only be bent but not compressed, each segment can be controlled with two degrees of freedom. An external motion

*The training time is recorded on a desktop workstation with an Intel i9-12900K CPU and an NVIDIA RTX 4090 GPU. The algorithm is fully implemented on the GPU. The workstation communicates through ROS with an onboard computer, which executes the control loop.

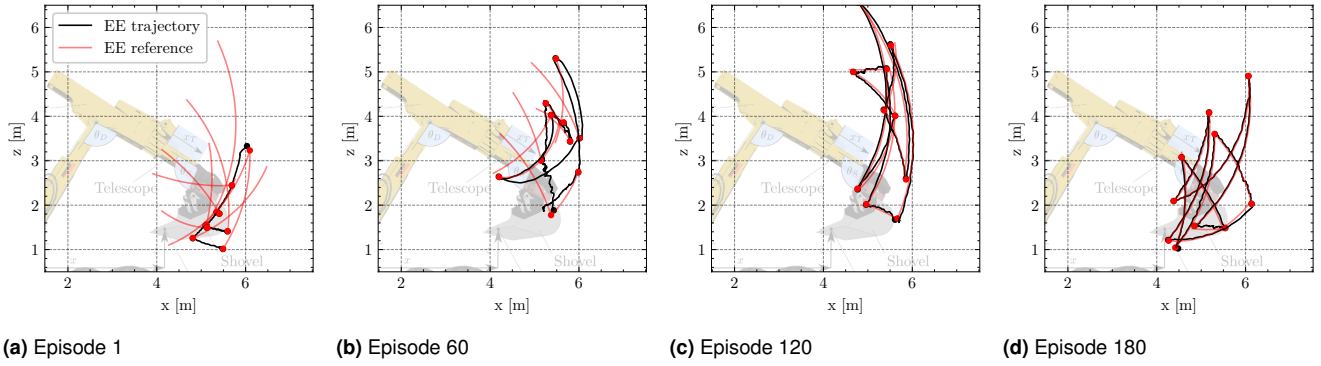


Figure 6. Real-world deployment results on the HEAP excavator at different training episodes. The plots show the tracking performance and adaptation over time.

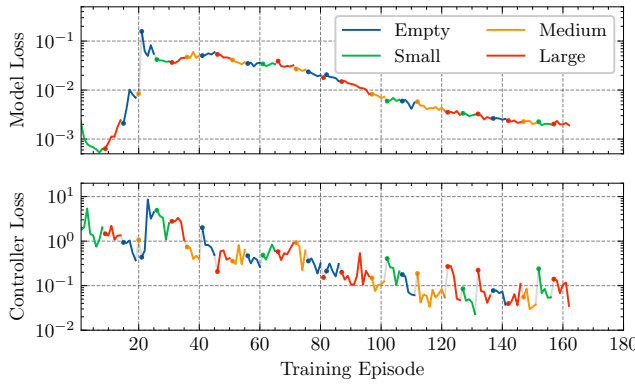


Figure 7. Online learning on HEAP with changing payload conditions. The plots show loss evolution with different colors showing episodes collected under different payload conditions. The first episode after each payload change is highlighted with a dot.

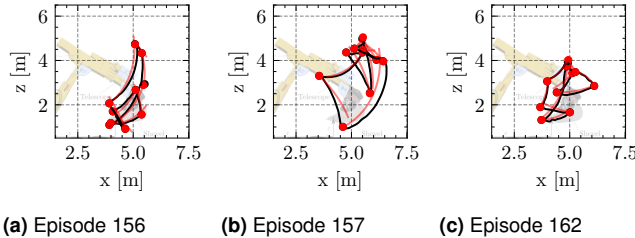


Figure 8. An example of online learning on HEAP with changing payload conditions. The plots show the tracking performance at (a) episode 156 with a small rock payload, (b) episode 157 right after switching to a large rock payload, and (c) episode 162 after a few episodes of adaptation.

capture system is used to track the poses of the ends of the helicoid segments.

We use the proposed online learning algorithm to train a control policy that steers the tip of the robot arm to follow a desired trajectory in the xy -plane. The learned model tries to predict the change in position of the end of the helicoid segments at the next time step, taking the state defined as the position of each helicoid segment's end. During training, the reference trajectories are randomly generated as polynomial curves with continuous velocity profiles, and the control policy predicts the desired motor position command for two motors of each segment. The third motor of each segment is



Figure 9. The cable-driven soft robot arm used in the experiments.

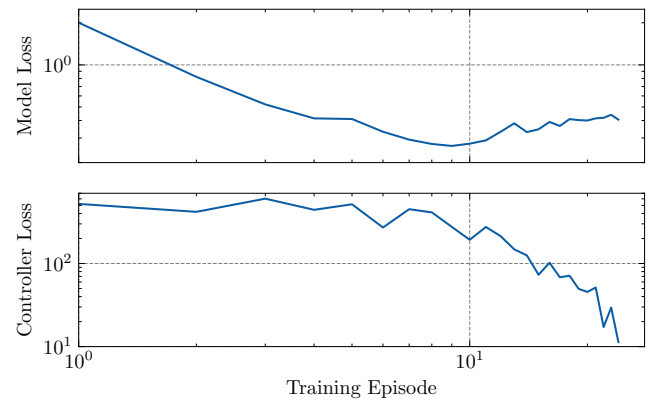
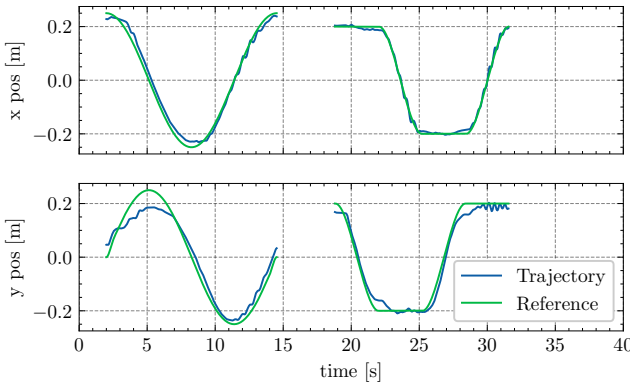
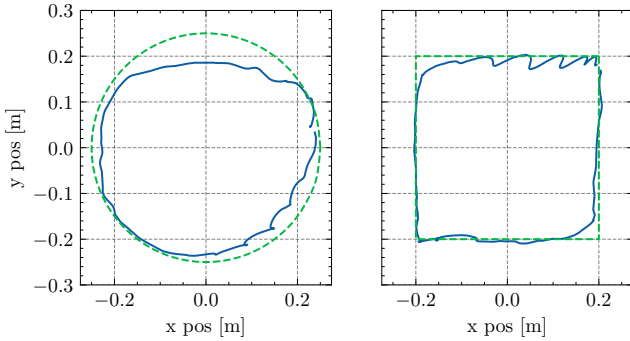


Figure 10. Convergence of the online model-based RL algorithm on the soft robot arm.

controlled to maintain the centerline length constant. Similar to the previous experiments, each episode consists of 10 trajectories, each lasting for 6 seconds.



(a) Reference and executed trajectory in x - and y -direction over time.



(b) Reference and executed trajectory in the xy -plane.

Figure 11. Tracking performance of the control policy on the soft robot arm. The top plot shows the trajectory in the xy -plane over time, while the bottom plot shows the trajectory in the xy -plane.

The online learning algorithm converges on the soft arm control task rapidly, reaching satisfactory performance in about 30 episodes. The loss plots of the training are shown in Figure 10. After 20 training episodes, the control policy is able to follow a desired trajectory reasonably well. The tracking performance on a circle and a square test trajectory is shown in Figure 11. The average tracking error is 2.95 cm. In comparison, previous work using a learned dynamics model and model-based control (Chen et al. 2024a) achieves a similar performance on similar trajectories.

Discussion

This work demonstrates an alternative approach to controlling robotic systems without using a simulator. Instead of relying on a sim-to-real strategy, the presented algorithm learns a control policy directly on the real robot. The algorithm relies on little prior knowledge, data, or modeling of the system. In fact, for the presented experiments on the hydraulic excavator and the soft arm, the learning algorithm was initialized in exactly the same way, with the only difference being the dimensions of the state and action spaces, and different normalization factors, as the state and action spaces have very different scales. By training the control policy solely with real robot data, we gain the additional benefit of not getting control policies biased on a potentially inaccurate simulator, an effect that is often observed in sim-to-real approaches. During online learning, if the model is

biased, the control policy can exploit the model's errors, collecting new data that updates the model to correct the bias.

The possibility to learn directly on the real robot was not possible due to the sample and computation efficiency of previous approaches. While model-based RL methods are already shown to be more sample efficient than model-free methods, previous approaches like MBPO (Janner et al. 2019), Dreamer (Wu et al. 2023), or TD-MPC (Hansen et al. 2024) require massive rollouts in imagination to perform zeroth-order policy or trajectory optimization. On the contrary, we combine model-based RL with differentiable RL techniques, which allows us to perform first-order policy optimization with the learned model. As a result, we can perform online learning on the real robot with hours of data while keeping the computational overhead low.

We justify the algorithm design with a theoretical analysis, which interprets the proposed algorithm as two online learning problems. The difference from standard online learning problems with i.i.d. data and loss gradients suggests the need for the proposed regularization techniques.

However, the presented algorithm is not without limitations. The theoretical analysis currently assumes that the data distribution shift is bounded. While this has been true in our experiments, the actual data distribution shift is a consequence of the control policy being updated, assuming a time-invariant robot dynamics and a stationary task distribution. The control policy update, on the other hand, is based on the model that is updated online. Therefore, the separate discussion of the two components does not consider the full complexity of the problem. A rigorous analysis that considers the overall stability of such online model learning would be a valuable addition to the theoretical analysis, not only to guarantee the stability of our algorithm, but also to serve as a general framework for analyzing model-based RL algorithms as well. This could be performed by using similar analysis for related problem settings, such as performatice prediction (Hardt and Mendler-Dünner 2025; Perdomo et al. 2020) and decision-dependent stochastic optimization (He et al. 2025).

In this project, we focused on trajectory-tracking tasks for robots with continuous control. While this is a common task with many use cases, many complex robotic tasks are described by discrete or sparse reward functions, such as grasping or manipulation tasks. Many manipulation tasks are also contact-rich, which can lead to discontinuous dynamics. To apply the proposed algorithm to such tasks, it is necessary to extend the proposed algorithm to use a latent state representation, similar to the implementation of Dreamer (Hafner et al. 2019b). In such complex tasks, the option to train from scratch on the real robot also needs to be reconsidered, as we have not evaluated the proposed algorithm on such tasks. Different pretraining strategies could be used to initialize the model, the control policy, or both. Expert demonstration data could also be added to the data buffer to accelerate model learning in the task distribution.

Finally, outliers and noise in the data can have a significant impact on the online learning algorithm. While learning in a simulation environment might be affected by the bias of the simulator, learning on the real robot is unavoidably affected by noise and outliers in the data. The noisy data leads to a

high-variance gradient estimate for both model and control policy training. While the issue in model training could be mitigated by using a growing mini-batch size over the accumulating data buffer, the control policy update, which is based on the limited on-policy data, is more sensitive to noise.

Conclusion

In this paper, we propose a model-based RL algorithm for learning to control robots directly on the real system. The algorithm combines online model learning from common model-based RL algorithms with analytical policy gradient updates, which allows for sample-efficient online learning. We justify the convergence of the algorithm from the perspective of an online optimization problem, and discuss how the analysis relates to other model-based RL and analytical policy gradient algorithms.

We evaluate the proposed algorithm on two distinct robotic systems that have modeling and control challenges: a hydraulic excavator arm and a cable-driven soft robot. The online learning algorithm was deployed on both systems, without any prior knowledge of the system dynamics or control policy, and achieves comparable performance to previously developed methods that rely on a complex workflow involving separate data collection, model learning, and controller design steps. The results show great potential for the proposed algorithm to be used in real-world robotic applications, by facilitating cross-embodiment transfer of control policies, in particular with robot systems with dynamics that are difficult to model.

Directions for future work include extending the algorithm to more complex tasks, such as manipulation tasks with discrete or sparse rewards, and to robot systems with discontinuous dynamics. On the theoretical side, the online learning analysis could be extended to consider the coupling between model learning and data distribution shift.

Acknowledgements

The authors would like to thank Mathieu Sandoz, Riccardo Maggioni, and Filippo Spinelli for their help with the experiment on HEAP, Cheng Pan for his help with the experiment on the soft arm, and Pascal Egli and Chenhao Li for their helpful discussions.

Funding

This project has received funding from the European Union's Horizon Europe Framework Programme under grant agreement No 101070405 and from NCCR Automation. This project is also funded by ...

Supplemental material

The supplementary material of this paper can be found at ...

References

Algoryx Simulation AB (2025) AGX dynamics: Real-time multi-body simulation. Algoryx Simulation AB.

Bern JM, Schnider Y, Banzet P, Kumar N and Coros S (2020) Soft Robot Control With a Learned Differentiable Model. In: *2020 3rd IEEE International Conference on Soft Robotics (RoboSoft)*. pp. 417–423.

Bi T and D'Andrea R (2024) Sample-Efficient Learning to Solve a Real-World Labyrinth Game Using Data-Augmented Model-Based Reinforcement Learning. In: *2024 IEEE International Conference on Robotics and Automation (ICRA)*. pp. 7455–7460.

Bubeck S (2015) Convex Optimization: Algorithms and Complexity. *Foundations and Trends® in Machine Learning* 8(3-4): 231–357.

Büchler D, Guist S, Calandra R, Berenz V, Schölkopf B and Peters J (2022) Learning to Play Table Tennis From Scratch Using Muscular Robots. *IEEE Transactions on Robotics* 38(6): 3850–3860.

Chen Z, Guan Q, Hughes J, Menciassi A and Stefanini C (2024a) S2C2A: A Flexible Task Space Planning and Control Strategy for Modular Soft Robot Arms. *arXiv:2410.03483*.

Chen Z, Ren X, Bernabei M, Mainardi V, Ciuti G and Stefanini C (2024b) A Hybrid Adaptive Controller for Soft Robot Interchangeability. *IEEE Robotics and Automation Letters* 9(1): 875–882.

Chen Z, Renda F, Le Gall A, Mocellin L, Bernabei M, Dangel T, Ciuti G, Cianchetti M and Stefanini C (2025) Data-Driven Methods Applied to Soft Robot Modeling and Control: A Review. *IEEE Transactions on Automation Science and Engineering* 22: 2241–2256.

Egli P and Hutter M (2022) A General Approach for the Automation of Hydraulic Excavator Arms Using Reinforcement Learning. *IEEE Robotics and Automation Letters* 7(2): 5679–5686.

Faure F, Duriez C, Delingette H, Allard J, Gilles B, Marchesseau S, Talbot H, Courtecuisse H, Bousquet G, Peterlik I and Cotin S (2012) SOFA: A Multi-Model Framework for Interactive Physical Simulation. In: Payan Y (ed.) *Soft Tissue Biomechanical Modeling for Computer Assisted Surgery*. Berlin, Heidelberg: Springer. ISBN 978-3-642-29014-5, pp. 283–321.

Guan Q, Stella F, Della Santina C, Leng J and Hughes J (2023) Trimmed helicoids: An architected soft structure yielding soft robots with high precision, large workspace, and compliant interactions. *npj Robotics* 1(1): 4.

Ha D and Schmidhuber J (2018) Recurrent World Models Facilitate Policy Evolution. In: *Advances in Neural Information Processing Systems*, volume 31. Curran Associates, Inc.

Haarnoja T, Zhou A, Abbeel P and Levine S (2018) Soft Actor-Critic: Off-Policy Maximum Entropy Deep Reinforcement Learning with a Stochastic Actor. In: *Proceedings of the 35th International Conference on Machine Learning*. PMLR, pp. 1861–1870.

Hafner D, Lillicrap T, Ba J and Norouzi M (2019a) Dream to Control: Learning Behaviors by Latent Imagination. In: *International Conference on Learning Representations*.

Hafner D, Lillicrap T, Fischer I, Villegas R, Ha D, Lee H and Davidson J (2019b) Learning Latent Dynamics for Planning from Pixels. In: *Proceedings of the 36th International Conference on Machine Learning*. PMLR, pp. 2555–2565.

Hafner D, Lillicrap TP, Norouzi M and Ba J (2020) Mastering Atari with Discrete World Models. In: *International Conference on Learning Representations*.

Hafner D, Pasukonis J, Ba J and Lillicrap T (2025) Mastering diverse control tasks through world models. *Nature* 640(8059):

647–653.

Hansen N, Su H and Wang X (2024) TD-MPC2: Scalable, Robust World Models for Continuous Control. In: *The Twelfth International Conference on Learning Representations*.

Hansen NA, Su H and Wang X (2022) Temporal Difference Learning for Model Predictive Control. In: *Proceedings of the 39th International Conference on Machine Learning*. PMLR, pp. 8387–8406.

Hardt M and Mendler-Dünner C (2025) Performative Prediction: Past and Future. [arXiv:2310.16608](https://arxiv.org/abs/2310.16608).

Hazan E (2019) *Introduction to Online Convex Optimization*.

Hazan E and Singh K (2025) Introduction to Online Control. [arXiv:2211.09619](https://arxiv.org/abs/2211.09619).

He Z, Bolognani S, Dörfler F and Muehlebach M (2025) Decision-Dependent Stochastic Optimization: The Role of Distribution Dynamics. [arXiv:2503.07324](https://arxiv.org/abs/2503.07324).

Hofer M, Spannagl L and D’Andrea R (2019) Iterative Learning Control for Fast and Accurate Position Tracking with an Articulated Soft Robotic Arm. In: *2019 IEEE/RSJ International Conference on Intelligent Robots and Systems (IROS)*. Macau, China: IEEE. ISBN 978-1-7281-4004-9, pp. 6602–6607.

Janner M, Fu J, Zhang M and Levine S (2019) When to Trust Your Model: Model-Based Policy Optimization. In: *Advances in Neural Information Processing Systems*, volume 32. Curran Associates, Inc.

Jud D, Kerscher S, Wermelinger M, Jelavic E, Egli P, Leemann P, Hottiger G and Hutter M (2021) HEAP - The autonomous walking excavator. *Automation in Construction* 129: 103783.

Kadian A, Truong J, Gokaslan A, Clegg A, Wijmans E, Lee S, Savva M, Chernova S and Batra D (2020) Sim2Real Predictivity: Does Evaluation in Simulation Predict Real-World Performance? *IEEE Robotics and Automation Letters* 5(4): 6670–6677.

Kaufmann E, Bauersfeld L, Loquercio A, Müller M, Koltun V and Scaramuzza D (2023) Champion-level drone racing using deep reinforcement learning. *Nature* 620(7976): 982–987.

Kingma DP and Ba J (2015) Adam: A Method for Stochastic Optimization. In: Bengio Y and LeCun Y (eds.) *3rd International Conference on Learning Representations, ICLR 2015, San Diego, CA, USA, May 7-9, 2015, Conference Track Proceedings*.

Kroemer O, Niekum S and Konidaris G (2021) A Review of Robot Learning for Manipulation: Challenges, Representations, and Algorithms. *Journal of Machine Learning Research* 22(30): 1–82.

Kumar A, Fu Z, Pathak D and Malik J (2021) RMA: Rapid Motor Adaptation for Legged Robots. In: *Robotics: Science and Systems XVII*, volume 17. ISBN 978-0-9923747-7-8.

Lee M, Choi H, Kim C, Moon J, Kim D and Lee D (2022) Precision Motion Control of Robotized Industrial Hydraulic Excavators via Data-Driven Model Inversion. *IEEE Robotics and Automation Letters* 7(2): 1912–1919.

Li C, Krause A and Hutter M (2025a) Offline Robotic World Model: Learning Robotic Policies without a Physics Simulator. [arXiv:2504.16680](https://arxiv.org/abs/2504.16680).

Li C, Krause A and Hutter M (2025b) Robotic World Model: A Neural Network Simulator for Robust Policy Optimization in Robotics. [arXiv:2501.10100](https://arxiv.org/abs/2501.10100).

Li Y, Wang X and Kwok KW (2022) Towards Adaptive Continuous Control of Soft Robotic Manipulator using Reinforcement Learning. In: *2022 IEEE/RSJ International Conference on Intelligent Robots and Systems (IROS)*. pp. 7074–7081.

Liberzon D (2016) Nonlinear and Adaptive Control Lecture Notes. URL <https://liberzon.csl.illinois.edu/teaching/16ece517notes.pdf>. (accessed 2025-09-23).

Lillicrap TP, Hunt JJ, Pritzel A, Heess N, Erez T, Tassa Y, Silver D and Wierstra D (2015) Continuous control with deep reinforcement learning. [arXiv:1509.02971](https://arxiv.org/abs/1509.02971).

Lin T, Sachdev K, Fan L, Malik J and Zhu Y (2025) Sim-to-Real Reinforcement Learning for Vision-Based Dexterous Manipulation on Humanoids. [arXiv:2502.20396](https://arxiv.org/abs/2502.20396).

Lin Y, Preiss JA, Xie F, Anand E, Chung SJ, Yue Y and Wierman A (2024) Online Policy Optimization in Unknown Nonlinear Systems. In: *Proceedings of Thirty Seventh Conference on Learning Theory*. PMLR, pp. 3475–3522.

Ma H, Büchler D, Schölkopf B and Muehlebach M (2022) A Learning-based Iterative Control Framework for Controlling a Robot Arm with Pneumatic Artificial Muscles. In: *Robotics: Science and Systems XVIII*, volume 18. ISBN 978-0-9923747-8-5.

Ma H, Büchler D, Schölkopf B and Muehlebach M (2023) Reinforcement learning with model-based feedforward inputs for robotic table tennis. *Autonomous Robots* 47(8): 1387–1403.

Ma H, Zeilinger M and Muehlebach M (2024) Stochastic Online Optimization for Cyber-Physical and Robotic Systems. [arXiv:2404.05318](https://arxiv.org/abs/2404.05318).

Makoviychuk V, Wawrzyniak L, Guo Y, Lu M, Storey K, Macklin M, Hoeller D, Rudin N, Allshire A, Handa A and State G (2021) Isaac Gym: High Performance GPU-Based Physics Simulation For Robot Learning. [arXiv:2108.10470](https://arxiv.org/abs/2108.10470).

Mattila J, Koivumäki J, Caldwell DG and Semini C (2017) A Survey on Control of Hydraulic Robotic Manipulators With Projection to Future Trends. *IEEE/ASME Transactions on Mechatronics* 22(2): 669–680.

Miki T, Lee J, Hwangbo J, Wellhausen L, Koltun V and Hutter M (2022) Learning robust perceptive locomotion for quadrupedal robots in the wild. *Science Robotics* 7(62): eabk2822.

Nagabandi A, Kahn G, Fearing RS and Levine S (2018) Neural Network Dynamics for Model-Based Deep Reinforcement Learning with Model-Free Fine-Tuning. In: *2018 IEEE International Conference on Robotics and Automation (ICRA)*. pp. 7559–7566.

Nan F and Hutter M (2024) Learning Adaptive Controller for Hydraulic Machinery Automation. *IEEE Robotics and Automation Letters* 9(4): 3972–3979.

Nurmi J, M Aref M and Mattila J (2018) A Neural Network Strategy for Learning of Nonlinearities Toward Feed-Forward Control of Pressure-Compensated Hydraulic Valves With a Significant Dead Zone. In: *BATH/ASME 2018 Symposium on Fluid Power and Motion Control*. American Society of Mechanical Engineers Digital Collection.

Nurmi J and Mattila J (2017) Automated Feed-Forward Learning for Pressure-Compensated Mobile Hydraulic Valves With Significant Dead-Zone. In: *ASME/BATH 2017 Symposium on Fluid Power and Motion Control*. American Society of Mechanical Engineers Digital Collection.

Mechanical Engineers Digital Collection.

Perdomo J, Zrnic T, Mendler-Dünner C and Hardt M (2020) Performative Prediction. In: *Proceedings of the 37th International Conference on Machine Learning*. PMLR, pp. 7599–7609.

Pierallini M, Gopanunni RKM, Angelini F, Bicchi A and Garabini M (2025) Fishing for Data: Modeling, Optimal Planning, and Iterative Learning Control for Flexible Link Robots. *IEEE Transactions on Control Systems Technology* : 1–17.

Romero A, Shenai A, Geles I, Aljalbout E and Scaramuzza D (2025) Dream to Fly: Model-Based Reinforcement Learning for Vision-Based Drone Flight. [arXiv:2501.14377](https://arxiv.org/abs/2501.14377).

Sapai S, Loo JY, Ding ZY, Tan CP, Baskaran VM and Nurzaman SG (2023) A Deep Learning Framework for Soft Robots with Synthetic Data. *Soft Robotics* 10(6): 1224–1240.

Schulman J, Wolski F, Dhariwal P, Radford A and Klimov O (2017) Proximal Policy Optimization Algorithms. [arXiv:1707.06347](https://arxiv.org/abs/1707.06347).

Song Y, Kim S and Scaramuzza D (2024) Learning Quadruped Locomotion Using Differentiable Simulation. [arXiv:2403.14864](https://arxiv.org/abs/2403.14864).

Spinelli FA and Katzschmann RK (2022) A Unified and Modular Model Predictive Control Framework for Soft Continuum Manipulators under Internal and External Constraints. In: *2022 IEEE/RSJ International Conference on Intelligent Robots and Systems (IROS)*. pp. 9393–9400.

Sutton RS (1990) Integrated Modeling and Control Based on Reinforcement Learning and Dynamic Programming. In: *Advances in Neural Information Processing Systems*, volume 3. Morgan-Kaufmann.

The MathWorks Inc (2025) Simscape: Multidomain physical-system simulation. The MathWorks Inc.

Tobin J, Fong R, Ray A, Schneider J, Zaremba W and Abbeel P (2017) Domain randomization for transferring deep neural networks from simulation to the real world. In: *2017 IEEE/RSJ International Conference on Intelligent Robots and Systems (IROS)*. pp. 23–30.

Villasevil MT, Simeonov A, Li Z, Chan A, Chen T, Gupta A and Agrawal P (2024) Reconciling Reality through Simulation: A Real-To-Sim-to-Real Approach for Robust Manipulation. In: *Robotics: Science and Systems XX*, volume 20. ISBN 979-8-9902848-0-7.

Wu P, Escontrela A, Hafner D, Abbeel P and Goldberg K (2023) DayDreamer: World Models for Physical Robot Learning. In: *Proceedings of The 6th Conference on Robot Learning*. PMLR, pp. 2226–2240.

Zhang Y, Hu Y, Song Y, Zou D and Lin W (2025) Learning vision-based agile flight via differentiable physics. *Nature Machine Intelligence* 7(6): 954–966.

Appendix

Derivation of model learning regret

The model learning part of Algorithm 1 can be analyzed as an online learning problem with shifting data distribution. While the data distribution, induced by the updating policy, is in fact affected by the learned model, we perform the analysis of the model learning problem itself, isolated from the policy update. To do this, we could consider the model parameter update as an SGD process on a slowly growing

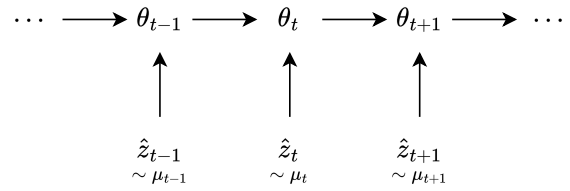


Figure 12. SGD update with shifting episode-wise data. Given the sequence $\{\mu_t\}$, draws $\hat{z}_t \sim \mu_t$ and $\hat{z}_{t+1} \sim \mu_{t+1}$ are independent conditioning on current parameters.

dataset, which has a predefined data distribution sequence unknown to the algorithm.

We first consider a variation of the standard SGD scheme, where the data distribution in each episode shifts. Let $\{\mu_t\}_{t \geq 1}$ be a sequence of data distributions. In our model learning case, it is defined on the space of state-action-next state triplets on $\mathcal{Z} = \mathcal{X} \times \mathcal{U} \times \mathcal{X}$. At episode t , a mini-batch element $\hat{z}_t \sim \mu_t$ is drawn and we perform one SGD step

$$\theta_t = \theta_{t-1} - \alpha \nabla_{\theta} \ell(\theta_{t-1}; \hat{z}_t).$$

The dependencies between the random variables \hat{z}_t and θ_{t-1} are illustrated in Figure 12. Due to the resampling of \hat{z}_t at each episode, there is no dependency between \hat{z}_t and \hat{z}_{t+1} conditioning on the model parameter θ_t .

Define the episode-wise optimal parameter w.r.t. the current data distribution

$$\theta_t^* \in \arg \min_{\theta} \mathbb{E}_{z \sim \mu_t} \ell(\theta; z),$$

and the episode-to-episode drift

$$\tilde{\Delta}_t \doteq \|\mu_t - \mu_{t-1}\|_{\text{TV}} \quad (t \geq 2), \quad \tilde{\Delta}_1 := 0.$$

We study the regret on model prediction loss w.r.t. the current data distribution,

$$\tilde{Y}_T \doteq \sum_{t=1}^T \underbrace{\left(\mathbb{E}_{z \sim \mu_t} \ell(\theta_t; z) - \mathbb{E}_{z \sim \mu_t} \ell(\theta_t^*; z) \right)}_{=: \tilde{Y}_t},$$

For any $t \geq 2$. We could decompose the optimality gap at episode t as

$$\begin{aligned} \tilde{Y}_t &= \underbrace{\mathbb{E}_{z \sim \mu_t} [\ell(\theta_t; z)] - \underbrace{\mathbb{E}_{z \sim \mu_{t-1}} [\ell(\theta_t; z)]}_{(I)_t}}_{(I)} \\ &\quad + \underbrace{\mathbb{E}_{z \sim \mu_{t-1}} [\ell(\theta_t; z) - \ell(\theta_{t-1}; z)]}_{(II)_t} + \underbrace{\tilde{Y}_{t-1}}_{(III)_t} \\ &\quad + \underbrace{\mathbb{E}_{z \sim \mu_{t-1}} [\ell(\theta_{t-1}^*; z) - \ell(\theta_t^*; z)]}_{(IV)_t \leq 0} \\ &\quad + \underbrace{\mathbb{E}_{z \sim \mu_{t-1}} [\ell(\theta_t^*; z)] - \mathbb{E}_{z \sim \mu_t} [\ell(\theta_t^*; z)]}_{(V)_t}. \end{aligned}$$

Since we assume the loss function ℓ is Lipschitz continuous on the compact set $\Theta \times \mathcal{Z}$, it attains a finite maximum (Extreme Value Theorem). Hence there exists

$$K \doteq \sup_{(\theta, z) \in \Theta \times \mathcal{Z}} |\ell(\theta; z)| < \infty.$$

Then, the drift pieces satisfy

$$|\text{(I)}_t| \leq 2K\tilde{\Delta}_t, \quad |\text{(V)}_t| \leq 2K\tilde{\Delta}_t,$$

by bounded loss and the TV inequality. For the other terms, we use the update rule $\theta_t = \theta_{t-1} - \alpha \nabla_{\theta} \ell(\theta_{t-1}; \hat{z}_t)$ with $\hat{z}_t \sim \mu_t$, β_L -smoothness, the second-moment bound, and PL:

$$\begin{aligned} & \mathbb{E}_{z \sim \mu_t} \ell(\theta_t; z) - \mathbb{E}_{z \sim \mu_t} \ell(\theta_{t-1}; z) \\ & \leq -\alpha \mathbb{E}_{z, \hat{z} \sim \mu_t} [\nabla_{\theta} \ell(\theta_{t-1}; z)^T \nabla_{\theta} \ell(\theta_{t-1}; \hat{z}_t)] \\ & \quad + \frac{\alpha^2 \beta_L}{2} \mathbb{E}_{\hat{z} \sim \mu_t} [\|\nabla_{\theta} \ell(\theta_{t-1}; \hat{z}_t)\|^2] \\ & = -\alpha \gamma \left(1 - \frac{\alpha \beta_L}{2}\right) \mathbb{E}_{z \sim \mu_t} [\ell(\theta_{t-1}; z) - \ell(\theta_t^*; z)] \\ & \quad + \frac{\alpha^2 \beta_L \sigma^2}{2} \frac{1}{B}, \end{aligned}$$

where γ is the PL constant. In the last step we use the standard assumption in SGD that the variance of the stochastic gradient is bounded by σ^2/B with mini-batch size B .

Therefore, we have

$$\begin{aligned} & \text{(II)}_t + \text{(III)}_t \\ & \leq -\alpha \gamma \left(1 - \frac{\alpha \beta_L}{2}\right) \mathbb{E}_{\mu_t} [\ell(\theta_{t-1}; z) - \ell(\theta_t^*; z)] \\ & \quad + \mathbb{E}_{\mu_{t-1}} [\ell(\theta_{t-1}; z) - \ell(\theta_t^*; z)] + \frac{\alpha^2 \beta_L \sigma^2}{2} \frac{1}{B}. \end{aligned}$$

Combining all the terms (I) to (V), and notice that $\mathbb{E}_{\mu_t} [\ell(\theta_{t-1}; z) - \ell(\theta_t^*; z)] - \mathbb{E}_{\mu_{t-1}} [\ell(\theta_{t-1}; z) - \ell(\theta_t^*; z)]$ can be bounded again by TV distance, we obtain a recursion for \tilde{Y}_t :

$$\begin{aligned} \tilde{Y}_t & \leq r\tilde{Y}_{t-1} + \frac{\alpha^2 \beta_L \sigma^2}{2} \frac{1}{B} + 4K\tilde{\Delta}_t + 4K(1-r)\tilde{\Delta}_t, \\ r & \doteq 1 - \alpha \gamma \left(1 - \frac{\alpha \beta_L}{2}\right). \end{aligned}$$

One can choose α small enough such that $\alpha \leq 1/\beta_L$ and $0 < r < 1$. Then $r \leq 1 - \alpha\gamma/2$, and the above recursion becomes

$$\tilde{Y}_t \leq r\tilde{Y}_{t-1} + \frac{\alpha^2 \beta_L \sigma^2}{2} \frac{1}{B} + 8K\tilde{\Delta}_t. \quad (16)$$

Unrolling (16) for $t \geq 2$ with $\tilde{Y}_1 \leq C$ gives

$$\tilde{Y}_t \leq 8K \sum_{\tau=2}^t r^{t-\tau} \tilde{\Delta}_\tau + r^{t-1} C + \sum_{\tau=2}^t r^{t-\tau} \frac{\alpha^2 \beta_L \sigma^2}{2} \frac{1}{B}.$$

Summing $t = 2$ to T and using $\sum_{s \geq 0} r^s \leq \frac{1}{1-r}$ yields

$$\sum_{t=2}^T \tilde{Y}_t \leq \frac{16K}{\alpha\gamma} \sum_{\tau=2}^T \tilde{\Delta}_\tau + \frac{2C}{\alpha\gamma} + \frac{\beta_L \sigma^2}{B} \cdot \frac{\alpha}{\gamma} T, \quad (17)$$

which bounds the total regret \tilde{R}_T .

The bound shown in (17) consists of three parts. If there is no distribution change in the learning process, the first term vanishes and the rest can be balanced by choosing $\alpha \propto 1/\sqrt{T}$ to recover the standard $O(\sqrt{T})$ rate. However,

the influence of the first term must be considered when the data distribution is shifting.

In the model learning setting of Algorithm 1, μ_t is the data distribution defined by uniformly sampling the buffered data in \mathcal{D}_t . Recall that we use Δ_t to denote the episode-to-episode drift of collected data distribution ν_t : $\Delta_t = \|\nu_t - \nu_{t-1}\|_{\text{TV}}$ for $t \geq 2$ and $\Delta_1 = 0$. By the triangle inequality,

$$\begin{aligned} \|\nu_t - \mu_t\|_{\text{TV}} & \leq \frac{1}{t} \sum_{i=1}^t \|\nu_t - \nu_i\|_{\text{TV}} \leq \frac{1}{t} \sum_{i=2}^t (i-1)\Delta_i, \\ \|\mu_t - \mu_{t-1}\|_{\text{TV}} & \leq \frac{1}{t} \|\nu_t - \mu_{t-1}\|_{\text{TV}} \\ & \leq \frac{1}{t(t-1)} \sum_{i=2}^t (i-1)\Delta_i. \end{aligned}$$

Then the first term of (17) can be bounded by an expression of Δ_i :

$$\sum_{\tau=2}^T \tilde{\Delta}_\tau = \sum_{\tau=2}^T \frac{1}{\tau(\tau-1)} \sum_{i=2}^{\tau} (i-1)\Delta_i \leq \sum_{\tau=2}^T \Delta_\tau$$

In Algorithm 1, we only care about the model loss on the latest episode of data, as we only calculate policy gradients based on the most recent data. Therefore, to analyze the model learning regret on

$$\begin{aligned} \bar{R}_T & \doteq \sum_{t=1}^T \left(\mathbb{E}_{z \sim \nu_t} \ell(\theta_t; z) - \mathbb{E}_{z \sim \nu_t} \ell(\theta_t^*; z) \right) \\ \theta_t^* & \in \arg \min_{\theta} \mathbb{E}_{z \sim \nu_t} \ell(\theta; z), \end{aligned}$$

we decompose it as

$$\begin{aligned} & \mathbb{E}_{z \sim \nu_t} \ell(\theta_t; z) - \mathbb{E}_{z \sim \nu_t} \ell(\theta_t^*; z) \\ & = \underbrace{\mathbb{E}_{\nu_t} \ell(\theta_t; z) - \mathbb{E}_{\mu_t} \ell(\theta_t; z)}_{(A)_t} + \underbrace{\mathbb{E}_{\mu_t} \ell(\theta_t; z) - \mathbb{E}_{\mu_t} \ell(\theta_t^*; z)}_{(B)_t = \tilde{Y}_t} \\ & \quad + \underbrace{\mathbb{E}_{\mu_t} \ell(\theta_t^*; z) - \mathbb{E}_{\mu_t} \ell(\theta_t^*; z)}_{\leq 0} + \underbrace{\mathbb{E}_{\mu_t} \ell(\theta_t^*; z) - \mathbb{E}_{\nu_t} \ell(\theta_t^*; z)}_{(C)_t}. \end{aligned}$$

We bound the bridge terms again by TV distance and bounded loss:

$$(A)_t \leq 2K\|\nu_t - \mu_t\|_{\text{TV}}, \quad (C)_t \leq 2K\|\nu_t - \mu_t\|_{\text{TV}}.$$

Summing and plugging in Δ_t gives

$$\begin{aligned} \sum_{t=1}^T ((A)_t + (C)_t) & \leq 4K \sum_{t=1}^T \|\nu_t - \mu_t\|_{\text{TV}} \\ & \leq 4K \sum_{t=1}^T \frac{1}{t} \sum_{i=2}^t (i-1)\Delta_i. \end{aligned}$$

Combining (17) and the terms (A) and (C) yields

$$\begin{aligned} \mathbb{E}[\bar{R}_T] & \leq 4K \sum_{t=1}^T \frac{1}{t} \sum_{i=2}^t (i-1)\Delta_i + \frac{16K}{\alpha\gamma} \sum_{\tau=2}^T \Delta_\tau \\ & \quad + \frac{2C}{\alpha\gamma} + \frac{\beta_L \sigma^2}{B} \cdot \frac{\alpha}{\gamma} T, \end{aligned}$$

which is the same form as (15).